Optimization study of octane-in-water emulsions by sedimentation field-flow fractionation

MARCIA E. HANSEN[*,a] and DAVID C. SHORT

The Procter & Gamble Company, Packaged Soap and Detergent Division, 5299 Spring Grove Avenue, Cincinnati, OH 45217 (U.S.A.)

ABSTRACT

The droplet size distributions of octane-in-water emulsions have been studied by sedimentation field-flow fractionation (SdFFF). Initially, the experimental parameters of the SdFFF experiment were examined to optimize these conditions for an octane emulsion stabilized by sodium dodecyl sulfate (SDS). The carrier flow-rate had a large impact on sample recovery. Resolution of the various size species was optimized by using the appropriate field strength and relaxation parameters. Comparison of the SDS emulsion to a similar SDS emulsion with added sodium chloride and to an non-ionic system, Brij 35, confirmed the sensitivity of the SdFFF method to differences in size distribution. Examination of the droplet size distribution over a 70-h period provided insights into the stability of these systems.

INTRODUCTION

In order to characterize the efficiency of surfactants in stabilizing oil droplets in solution, we developed a method for monitoring oil droplet size distributions. We expected that information about the initial droplet size and the demulsification kinetics of oil-in-water emulsions would provide insights into the structure of the surfactant–oil interface as well as the overall performance of each individual surfactant system in suspending oil droplets in aqueous solutions. As a first approach, we chose *n*-octane as a model oil and studied *n*-octane emulsions as prepared by ultrasonic dispersion of octane in the presence of simple surfactant systems. These surfactant systems included anionic and non-ionic surfactants. Specifically, sodium dodecyl sulfate (SDS) and Brij-35 (a polyethylene glycol ether of lauryl alcohol) systems at concentrations slightly above their critical micelle concentrations (CMC) were studied. The effect of salt in the anionic surfactant system was also investigated. The sonication of octane in the presence of surfactant was expected to generate a system of large oil

---

[a] Present address: FFFractionation, Inc., P.O. Box 58718, Salt Lake City, UT 84158-0718, U.S.A.

droplets, formally termed a macro-emulsion. Differences in the packing of surfactant molecules at the surfactant–octane interface should lead to differences in the droplet size resulting from sonication. Also, the physical structure of the surfactant–octane interface should be reflected by the stability of the system of oil droplets against demulsification into larger droplets.

For the analysis of the oil droplet size distributions, a sedimentation field-flow fractionation (SdFFF) technique was optimized. This technique has been extensively used for the determination of particle size distributions of latex particles[1,2]. Since oil droplets are more delicate than typical particle samples, we could not assume that this sample would behave as a "hard sphere". Therefore, in this study, we report the optimization of the experimental parameters of the SdFFF technique, such as the field strength, the carrier flow-rate, relaxation time, and injection method.

SdFFF is a high-resolution particle sizing technique, which separates sample species according to their buoyant mass. This technique has been described in great detail elsewhere[1]. Basically, in SdFFF a centrifugal field is imposed perpendicularly across a thin, open flow channel. SdFFF channels are typically 80 cm × 2.0 cm × 0.025 cm. Sample species are deposited in zones of a characteristic thickness according to their interaction with the field. The buoyant mass of the sample species and the centrifuge rpm and rotor radius determine the sample–field interaction. The laminar flow profile across the thin dimension of the channel allows sample species to be differentially eluted due to their varying zone thicknesses. In the case of emulsions, the larger, more buoyant oil droplets form a more compressed sample zone near the upper channel wall. This sample zone is eluted after the less dense sample zones of smaller droplets.

SdFFF is potentially superior to competing particle sizing methods for the analysis of emulsions. This technique was applied to commercial emulsions of safflower and soybean oils by Yant et al.[3]. The buoyancy of the sample causes no problem, as in other methods; oil droplets are deposited at the top channel wall, but are fractionated just like the particles with negative buoyancy which are deposited at the bottom wall. Light-scattering and centrifugal techniques[4,5] have been most commonly applied to the study of emulsion droplet size. However, as samples must not be stirred for light-scattering measurements, results are possibly biased due to the differential float-rate of the droplets of varying diameter. Also, analysis of emulsions with general centrifugal techniques is difficult as these systems are designed for particles heavier than the suspension media. Alternatively, application of microscopic techniques to the sizing of emulsion droplets is cumbersome and droplets below 0.5 μm are not readily detected. With SdFFF it is additionally possible to obtain true distribution data, as opposed to the mean diameter and polydispersity data provided by light-scattering techniques. Sample species are separated into mass-based fractions in SdFFF. Following separation, the turbidimetric response of a UV detector individually quantifies each fraction.

Another advantage of the SdFFF separation scheme is the inherent flexibility of the system. Retention of a sample may be fine-tuned by adjusting the centrifuge speed. Increased retention yields greater resolution between particles of similar diameter, although experiment run time is concomitantly increased. Offset of the time factor may be accomplished by increasing carrier flow-rate.

The trends described above hold only for the idealized "hard-sphere" particle

sample. For the delicate type of sample studied in this report, increases in field strength and flow-rate may adversely affect the integrity of the droplets. At higher field strengths the zone thickness of the sample is decreased. The zone is concentrated and compressed towards the channel wall so that there is a danger of oil droplets coalescing or sticking irreversibly to the channel wall. At increasing flow-rates, shearing the oil droplets is risked. Alternatively, higher flow-rates may encourage total recovery of sample as the droplets attached to the channel wall are dislodged. The present study examines these trade-offs between field strength and flow-rate conditions with the ultimate goal of producing optimal size distribution data in the shortest time under conditions that maintain the integrity of the oil droplets.

EXPERIMENTAL

Instrumentation
    The SdFFF unit used was a DuPont SF³ 2000 which is similar to the systems described previously[2,6], except for the data station. For this upgraded model an IBM computer and software are used. Otherwise, the instrumental components are the same as in other sedimentation field-flow fractionators[3]. Typically, the instrument consists of the SdFFF channel which fits inside a centrifuge, a high-performance liquid chromatography-type pump, and a UV detector set at 254 nm. The channel length and width were 56 and 2.5 cm, respectively. The channel volume, 2.92 ml, was measured using the retention time of a non-retained marker eluted at low flow-rate. The channel thickness, 0.021 cm, was calculated using the channel volume, length, and width measurements.

Methods
    The carrier composition used for the elution of the emulsion sample was identical to the surfactant system used in generating the emulsion, unless otherwise noted. Doubly distilled water was equilibrated with octane prior to the addition of the appropriate surfactant and salt. After the surfactant was thoroughly dissolved, the carrier solution was vacuum-filtered through a 0.22-μm filter. The carrier was sparged with helium.
    The octane emulsions were prepared using the method described by Avranas *et al.*[7]. A 5-ml portion of octane was added to 25 ml of the surfactant system prepared as described above. Emulsions were generated with a sonic probe (Branson Model 184V ultrasonic power supply with a Branson Model A410 watt meter), operating at 1000 W and 20 000 KHz under an atmosphere of nitrogen.

THEORY AND CALCULATIONS

Retention equations
    As the theoretical aspects of retention in SdFFF have been adequately explored and reported earlier[1], we will only briefly discuss those aspects of SdFFF pertinent to this study. In normal SdFFF, sample particles interact with the externally imposed sedimentation field so as to form zones with an exponential profile according to the following equation

$$c = c_0 \exp(-x/l) \tag{1}$$

where c is the concentration of particles at a distance x from the channel wall, c_0 is the concentration at the wall, and l is the mean zone thickness. The critical retention parameter, λ, is the ratio of l to the full channel thickness, w, and is related to the thermal energy, kT, and the force, F, exerted on a particle

$$\lambda = l/w = kT/Fw \tag{2}$$

The experimentally observed retention ratio (R) is related to λ as follows

$$R = 6\lambda[\coth(1/2\lambda) - 2\lambda] \tag{3}$$

Eqn. 3 is commonly simplified[3] to

$$R = 6\lambda - 12\lambda^2 \tag{4}$$

We further define λ in eqn. 5 so that the particle diameter, d, may be calculated from the observed retention ratio from the field strength, G, as determined by using the angular speed, ω, and rotor radius, r_r, of the centrifuge, and with $\Delta\rho$, the absolute difference between carrier and particle density. Particles are assumed to be spherical.

$$\lambda = 6kT/(d^3\pi\Delta\rho\omega^2 r_r w) \tag{5}$$

The retention equation, eqn. 3, assumes particles to be point spheres with no hydrodynamic interaction due to physical size. When this consideration is added, the retention equation becomes more complicated. The sterically corrected retention equation has been expressed[8] as follows

$$R = 6\gamma(\alpha - \alpha^2) + 6\lambda(1 - 2\alpha)\{\coth[(1 - 2\alpha)/2\lambda] - 2\lambda/(1 - 2\alpha)\} \tag{6}$$

where $\alpha = d/2w$ and γ is a dimensionless factor with dependence on flow-rate, field strength, and particle diameter[9].

In sterically corrected SdFFF theory, the retention volume increases with particle diameter until the steric effect dominates. At this steric inversion point, there is a foldback in elution order. Particles larger than those eluted at the inversion point are eluted earlier under the dominating steric influences.

Relaxation calculation

Relaxation time, t_r, is the time required for each sample species to come to equilibrium in its respective zone. The velocity with which a sample particle travels from the far channel wall to the accumulation wall may be calculated by means of the classical Svedberg equation

$$\text{velocity} = (1 - v_1\rho)mG/f = (4/3)\pi\Delta\rho r_p^3 G/f \tag{7}$$

in which v_1 is the partial molar volume of the sample particle, m is the particle mass, r_p is the particle radius, and f is the frictional coefficient. Since the particle must travel the

distance of the channel thickness, w, we calculate the relaxation time, t_r, by using the Stoke's approximation for the friction coefficient.

$$t_r = 18\eta w/(\Delta\rho d^2 G) \tag{8}$$

The viscosity of the carrier solution is represented by η.

Peak dispersion calculations

Peak dispersion in SdFFF has been characterized in terms similar to that of liquid chromatography[1]. Plate height, H, which is variance, σ^2, per channel length, L, is expressed by

$$H = 2D/R[v] + \chi w^2[v]/D + \Sigma H_i \tag{9}$$

where D is the diffusion coefficient of the sample particles, $[v]$ is the average carrier linear flow velocity, χ is a non-equilibrium term as described below, and H_i includes all other miscellaneous contribution to peak dispersion, such as sample injection effects, channel irregularities, and dead volume effects. χ is a complicated term, but in the limit of high retention, this factor is reduced to a simple function of

$$\chi = 24\lambda^3 \tag{10}$$

RESULTS AND DISCUSSION

Optimization of experimental parameters

In general, we found that the octane emulsions, as generated by sonic dispersion, had bimodal particle size populations. These emulsions were unstable in that the size distribution changed with time. Initially, the emulsions had a single mode of smaller droplets which grew into larger droplets. In order to track this aging process, we optimized the SdFFF method so that the broad size range of droplets could be monitored under a single set of conditions, *i.e.* field strength, flow-rate, and relaxation time. At the lower end of the distribution, sufficient relaxation time and field strength were required to allow resolution of the small particles from the void. Optimization for the larger particles present in the distribution required a minimization of field strength or retention so that sample recovery was acceptable and analysis time was not excessive. A retention range of $R = 0.15$–0.05 has been recommended for optimum recovery and accuracy in the analysis of polystyrene lattices[10]. We used these limits as a guideline for our optimization study.

Optimization of field strength

As relaxation time is strongly dependent on field strength, we first scanned a range of centrifuge speeds to determine the optimum for the expected oil droplet size range. Assuming the density of the oil droplets at 0.7, the density of *n*-octane, we approximated an initial rpm for beginning the scan. Using a limiting upper diameter of 1 μm and a minimum retention ratio of 0.05, we calculated from eqns. 4 and 5 a field strength of 2.39 g, which requires a centrifuge speed of 150 rpm.

In Fig. 1 we compare the resolution and retention obtained by scanning from 150
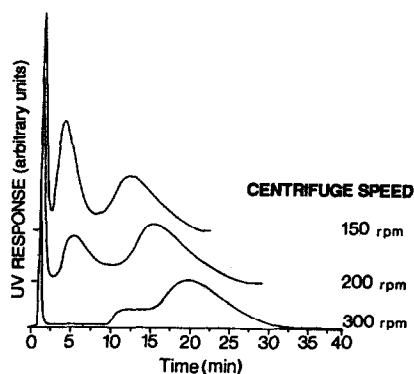
Fig. 1. Fractograms illustrating the effect of varying field strengths. Surfactant system, 0.3% SDS; emulsion age, 20 h; carrier flow-rate, 3.0 ml/min.

to 300 rpm at 3.0 ml/min using a 20-h-old octane-in-0.3% SDS emulsion. At this age, the emulsion has an intermediate range of particle size as will be discussed in the last section. At 300 rpm, the retention of the larger mode of particles is excessive at $R = 0.040$. At 150 rpm, the resolution between the void and first peak is just sufficient, but for younger emulsions with smaller particles, this level of resolution would not be acceptable. We continued the remainder of our optimization study at a centrifuge speed of 200 rpm. At this field strength (4.25 g), the retention ratios of the first and second modes of the bimodal size distribution are 0.15 and 0.060, indicating droplet diameters of 0.503 and 0.699 μm, respectively.

The possibility of sample degradation due to the concentrating effects of the centrifugal field could not be entirely eliminated. As a partial check, a 20-h-old emulsion was split into two portions and one of the portions was exposed to a centrifugal field of approximately 5 g for a period of 1 h. The resulting fractograms for analysis of these two sampels at 4.25 g, 3.0 ml/min, were compared and no significant differences were noted.

Optimization of relaxation time

Resolution of the smallest mode of particles from the void peak is dependent on a sufficient relaxation time. The void peak in SdFFF contains non-retained molecular components as well as very large particles which are eluted quickly due to steric effects and small particles not completely at equilibrium in their characteristic sample zone. The smallest droplet diameter of the 20-h sample mentioned above was 0.45 μm so that a 25-min relaxation time is required at a centrifuge speed of 200 rpm. However, we stressed the optimization of relaxation time by examining a fresh 1-h-old emulsion. Hypothetically, this sample had the smallest droplet. The droplet growth processes of the emulsion were presumably quenched by dilution at injection. Scanning from a relaxation time of 5 to 60 min, the dramatic effects of relaxation are evident (Fig. 2). Resolution between the void and the first size modes of droplets increases as the relaxation time is increased from 5 up to 45 min. In our opinion, the slight gain in resolution obtained by increasing the relaxation time from 45 to 60 min is not worth the extra analysis time. No loss in recovery, as determined by measuring the peak area, was observed by increasing the relaxation time.
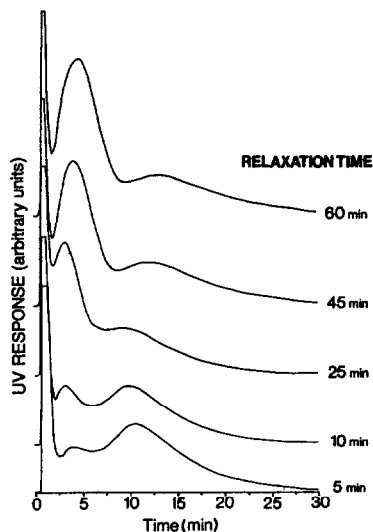
Fig. 2. Fractograms resulting from use of varying relaxation times. Surfactant system, 0.3% SDS; emulsion age, 1.0 h; field strength, 4.25 g; carrier flow-rate, 3.0 ml/min.

Injection flow-rate optimization

In the DuPont SF[3] 2000 system the sample is introduced via an injection valve, connected to the head of the SdFFF channel with approximately 80 cm of polystyrene tubing, at a volume of 0.55 ml. The flow-rate for the injection process is an optional parameter. It is automatically continued so until a total of 1.1 ml is washed through the injection valve and connecting tubing. The centrifuge field is on during sample injection so that sample begins relaxation as it enters the channel and theoretically does not travel an appreciable distance down the channel during the injection period. The default injection flow-rate in the SF[3] 2000 is 0.1 ml/min. This low flow-rate should minimize the migration of sample down the channel, but allow for band broadening in the 0.55 ml of tubing.
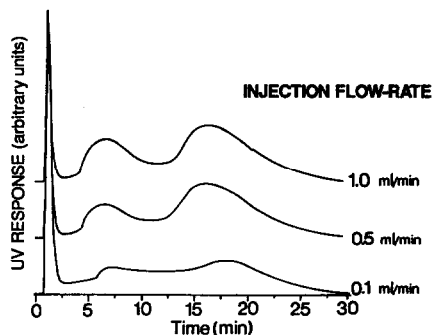

Fig. 3. Fractograms resulting from the use of varying injection flow-rates. Surfactant system, 0.3% SDS; emulsion age, 20 h; field strength, 4.25 g; carrier flow-rate, 3.0 ml/min.
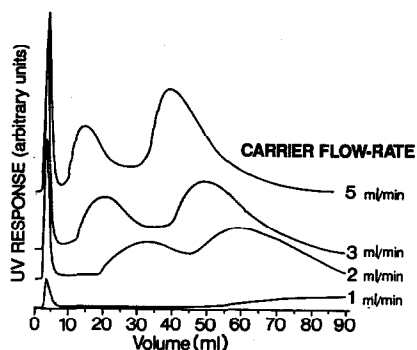
Fig. 4. Fractograms illustrating effect of varying carrier flow-rate on retention, resolution, and sample recovery. Emulsion age, 20 h; field strength, 4.25 g; relaxation time, 25 min.

When the injection flow-rate was varied, only a slight decrease in peak broadening with increasing flow-rate was observed (Fig. 3). The peak position did not shift appreciably with increasing flow-rate, indicating that sample migration down the channel during the injection process is not significant. The overall effect observed for increased flow injection velocities was increased recovery, implying that the sample sticks to the polystyrene tubing when the injection is slower. To minimize analysis time and maximize recovery we used an injection flow-rate of 1.0 ml/min.

Carrier flow-rate optimization

The final experimental parameter studied was carrier flow-rate. Obviously, analysis time is decreased with higher flow-rates. Potentially, sample recovery increases with flow-rate. However, from the plate-height equation, we calculated an increase in peak broadening and, thus, a decrease in resolution with increasing carrier velocities. Also, shearing of sample droplets may be induced at higher flow-rates. More importantly, the steric transition point is approached more rapidly with faster flow-rates. As these hydrodynamic steric effects are not sufficiently characterized at this time, the accuracy of the particle diameter calculation suffers. In the extreme case in which the particle diameter exceeds the diameter at the steric transition point, the foldback of retention leads to total confusion in the calculation of the size distribution[9].

In Fig. 4 the fractograms for various carrier flow-rates are compared on the basis of volume rather than time. This allows direct comparison and makes the effect on retention, peak broadening, and sample recovery obvious. A decrease in retention was noted as the carrier velocity was increased. This is explained by steric effects. The hydrodynamic lift forces that oppose normal retention mechanisms accelerate sample elution. The observed trend in peak width opposed the effect predicted by the plate height equation (eqn. 9). Plate heights measured from the two peaks of the bimodal population decreased with carrier velocity. Presumably, steric effects interfere with the normal peak broadening effect. Also, at larger carrier velocities the chromatographic effect of sample reversibly adhering to the channel wall is reduced. In the absence of this process, peak broadening is minimized.

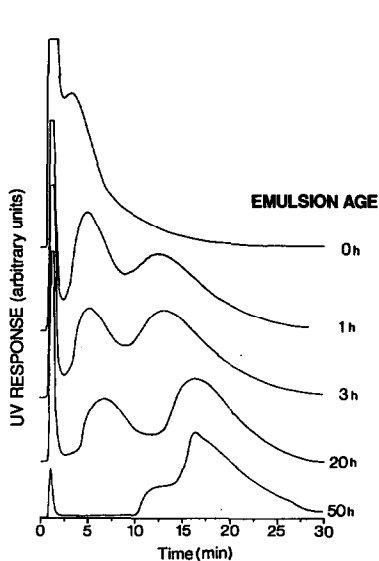An increase in recovery with flow-rate was also noted. The poor recovery and

Fig. 5. Fractograms for emulsions of octane in 0.3% SDS at varying ages. Field strength, 4.25 g; carrier flow-rate, 3.0 ml/min; relaxation time, 45 min; injection flow-rate, 1.0 ml/min.
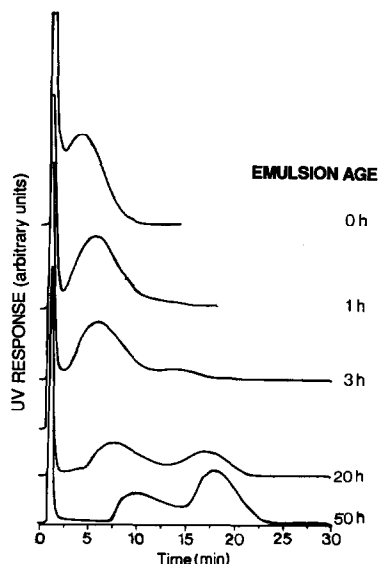
Fig. 6. Fractograms for emulsions of octane in 0.3% SDS with 0.2% sodium chloride at varying ages. Field strength, 4.25 g; carrier flow-rate, 3.0 ml/min; relaxation time, 45 min; injection flow-rate, 1.0 ml/min.

excessive retention at a flow-rate of 1.0 ml/min illustrates the definite advantage of using higher flow-rates to dislodge the sample. The previous set of experiments for optimizing the injection flow-rate further validate this effect. As a compromise between the advantages of higher flow-rates and the problems of steric effects induced at elevated flow-rates, an intermediate flow-rate, 3.0 ml/min, was chosen for the study of the dynamics of the octane emulsions.

Effect of surfactant system on the size distribution of octane-in-water emulsions

The sensitivity of the SdFFF method, as optimized above, was tested by examining the droplet size distribution of octane emulsions prepared in three different surfactant sytems. Two anionic systems at 0.3% SDS and 0.3% SDS with 0.2% sodium chloride, and a non-ionic system, 0.10% Brij 35, the polyethylene glycol ether of lauryl alcohol, $CH_3(CH_2)_{10}CH_2(OCH_2CH_2)_{23}OH$, were studied. These surfactant concentrations are slightly above the CMC of each system. The fractograms so obtained were reproducible for emulsions of similar age and composition. Carrier composition was found to affect the analysis. Emulsions generated in the presence of 0.3% SDS with 0.2% sodium chloride, but analyzed in a saltless carrier behaved similar to the emulsions generated and analyzed in solutions without sodium chloride. Possibly, the effects noted with salt are reversible.

The surfactant systems aged similarly, with a few notable differences (*cf.* Figs. 5–7). In all cases, the emulsions appeared to be dynamic: droplet diameter distributions changed with sample age. The most dramatic effects were noted in the first several hours. Immediately following sonication, the emulsions showed a monomodal size
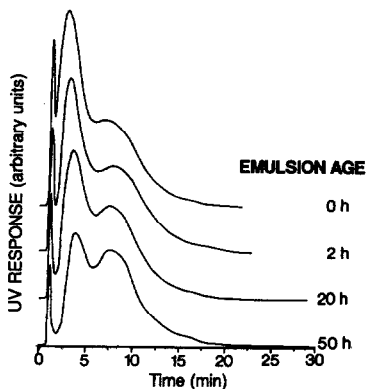
Fig. 7. Fractograms for emulsion of octane in 0.1% Brij 35 at varying ages. Field strength, 4.25 g; carrier flow-rate, 3.0 ml/min; relaxation time, 45 min; injection flow-rate, 1.0 ml/min.

population. A second mode of oil droplet diameters generally developed within the 3 h.

For the surfactant system with 0.3% SDS plus 0.2% sodium chloride, only a small amount of the second population developed in 3 h. The 0.1% Brij 35 system, on the other hand, showed a bimodal population immediately, but thereafter changed less rapidly with time than the other surfactant systems. Superior performance of the Brij system in stabilizing oil droplet is implied by the slower kinetics of droplet growth. According to a similar line of reasoning, the addition of sodium chloride to the 0.3% SDS solution increases the stability of the emulsion system: the small mode of droplet diameters is apparently more resistant to droplet growth. The current models for emulsion instability due to droplet growth are coalescence and molecular diffusion of the oil through the surfactant barrier[4]. At this point, we cannot distinguish between these models.

Table I shows the droplet diameters calculated for a larger range of emulsion age using the sterically corrected retention equation with a constant γ of 1. Again, the

TABLE I

COMPARISON OF DROPLET DIAMETERS (μm) FOR VARIOUS OCTANE EMULSIONS *VER-SUS* EMULSION AGE

Field strength, 4.25 g; carrier flow-rate, 3.0 ml/min; relaxation time, 45 min; injection flow-rate, 1.0 ml/min.

Emulsion age (h)	0.3% SDS		0.3% SDS + 0.2% NaCl		0.1% Brij 35	
	1st Mode	2nd Mode	1st Mode	2nd Mode	1st Mode	2nd Mode
0	0.376	—	0.408	—	0.344	0.500
1	0.438	0.631	0.464	—		
2			0.471	—	0.365	0.524
3	0.448	0.643	0.474	0.661		
6	0.445	0.666	0.480	0.679		
20	0.503	0.699	0.522	0.716	0.379	0.516
50	0.627	0.709	0.580	0.738	0.396	0.522
70	0.641	0.721	0.580	0.740	0.404	0.522

results for the non-ionic Brij system are notably different from those of the anionic systems. Droplet diameters are smaller and more stable over the 70-h time span tested. Presumably, differences in the structure of the non-ionic micelle *versus* an anionic micelle generate these effects. The packing of non-ionic surfactant molecules around the octane droplet is possibly tighter than the packing of anionic surfactant molecules, and this may protect the droplets from coalescence. Alternatively, a thicker coat of surfactant may be a less penetrable barrier to molecular diffusion. The presence of salt in the SDS system initially led to larger droplets. We suggest that sodium chloride also changes the structure of surfactant packing in the micelle. The increase in ionic strength allows the surfactant to pack more closely, decreasing the curvature at the octane–SDS interface[5]. Thus the resulting droplet assumes a larger diameter.

CONCLUSIONS

In this optimization study the experimental parameters used in analyzing the droplet size distribution of octane emulsions were found to impact the results significantly. Additionally, the calculations and considerations needed to search for the optimum conditions were expressed. The major effect noted involved the flow-rates used and the implication on sample recovery.

Both carrier and injection flow-rate had to be optimized. Apparently, the octane emulsions tested adhere extensively to the surfaces of the channel wall and polystyrene tubing. Relaxation time of sample in the system was also crucial for the resolution of the lower end of the particle size distribution.

The surfactant systems tested with the optimized experimental parameters illustrated the sensitivity of this method to changes in the size distribution. Bimodal populations were prevalent. These types of distributions are difficult to characterize by light-scattering techniques. The non-ionic surfactant system studied, Brij 35, showed differences in droplet diameter as well as droplet growth dynamics. As opposed to the anionic SDS system, the diameter of droplets in the non-ionic system were smaller and changed less with emulsion age. A comparison of anionic surfactant systems with and without sodium chloride showed the theoretically expected differences in the micelle structure. The droplets were initially larger in the system with salt due to the closer surfactant packing possible in the presence of salt and the resulting decrease in curvature at the octane–surfactant interface. The emulsions generated with salt were also more resistant to particle growth. This substantiates the hypothesized thicker packing of surfactant molecules.

Overall, the study confirmed the feasibility of using SdFFF for the study of emulsion dynamics. Sensitivity to the two populations of droplet diameters was demonstrated. Analysis time was not so excessive that the dynamics of the changing system could not be observed.

REFERENCES

1 J. C. Giddings, F. J. F. Yang and M. N. Myers, *Anal. Chem.*, 47 (1975) 126.
2 J. J. Kirkland, W. W. Yau and W. A. Dorner, *Anal. Chem.*, 50 (1980) 1944.
3 F. S. Yang, K. D. Caldwell, M. N. Myers and J. C. Giddings, *J. Colloid Interface Sci.*, 93 (1982) 115.
4 H. M. Cheung, *Langmuir*, 3 (1987) 744.
5 M. L. Robbins, J. Bock and J. S. Huang, *J. Colloid Interface Sci.*, 126 (1988) 114.
6 J. J. Kirkland, S. W. Rementer and W. W. Yau, *Anal. Chem.*, 51 (1981) 1730.
7 A. Avranas, G. Stalidis and G. Ritzoulis, *Colloid Polym. Sci.*, 266 (1988) 937.
8 M. N. Myers and J. C. Giddings, *Anal. Chem.*, 54 (1982) 2284.
9 S. Lee and J. C. Giddings, *Anal. Chem.*, 60 (1988) 2328.
10 K. D. Caldwell and J. Lee, presented at the *First International FFF Symposium, Park City, UT, June 1988*.